Received: 22 July 2025 | Revised: 23 September 2025 | Accepted: 29 September 2025 | Published online: 17 December 2025

RESEARCH ARTICLE

Journal of Climbing and Walking Robots
2025, Vol. 00(00) 1-11
DOI: 10.47852/bonviewJCWR52026892

BON VIEW PUBLISHING

A Bio-inspired Climbing Robot with Directional Dry Adhesion for Reduced-Gravity Mobility

Motaz Hassan[1,2,*], Oluwafemi Fayomi[1], Joshua Faust[1], and Ajay Mahajan[1,2]

[1] *Department of Mechanical Engineering, The University of Akron, USA*

[2] *Department of Biomedical Engineering, The University of Akron, USA*

Abstract: This study presents a six-legged climbing robot equipped with gecko-inspired dry adhesives and a ball-joint foot mechanism designed for stable locomotion on inclined and vertical surfaces. Each leg has two degrees of freedom (hip swing and foot lift) controlled via a Raspberry Pi 4, PWM-driven microservos, and adaptive slip tracking through an MPU-6050. For directional adhesion, custom PDMS footpads were molded from 7 µm diffraction gratings, allowing shear-based attachment without external power. The robot was tested under full gravity and a simulated reduced-gravity gantry mechanism decomposed of gravitational force vectors. Experiments were performed across slip angles from 0° to 90° on smooth acrylic surfaces, and four-legged and six-legged configurations were compared. Results show that the six-legged robot consistently achieved greater displacement, velocity, and efficiency than the four-legged robot. At 0° slip, forward displacement was increased with adhesion by ~60% compared with that without adhesion (18.72 ± 0.5 cm vs. 11.68 ± 0.4 cm). At 90° under reduced gravity, the six-legged robot maintained 56.3 ± 8.0% efficiency, compared to 0% for the quadruped, confirming the role of redundant contact points in sustaining locomotion. However, at 10° slip, efficiency decreased below 42% due to inconsistency in detachment and limits of rigid foot conformity. These findings validate the role of increased contact points and distributed adhesion in supporting locomotion in complex gravitational environments, making the system suitable for planetary exploration and on-orbit servicing. Future work will incorporate compliant toe mechanisms, active peeling strategies, and closed-loop gait control to improve detachment, load sharing, and adaptive locomotion.

Keywords: gecko-inspired, hexapod, climbing robot, adhesion strength, climbing performance, reduced gravity

1. Introduction

More robots are deployed in hazardous environments such as outer space, nuclear facilities, and disaster zones where prolonged human presence is deemed unsafe or impossible. In space applications, for instance, robots must perform inspections, repairs, or sample collection on spacecraft exteriors or planetary surfaces, often in microgravity or vacuum conditions [1–4]. Similarly, terrestrial environments like collapsed buildings or chemical plants demand robots that can navigate vertical or inverted surfaces without relying on infrastructure [5–9]. However, despite the development of numerous robotic systems for these tasks, integrating mobile climbing robots into routine operations remains challenging, particularly in cases where reliable adhesion and mobility are required across unstructured, dynamic terrains [10]. Traditional solutions, such as suction systems or electro-adhesion, are limited in terms of versatility, energy efficiency, and adaptability to non-ideal surfaces. Magnetic systems fail on non-ferrous materials, suction requires smooth substrates and continuous power, and electro-adhesion struggles in dusty or humid environments [11–13]. These constraints are especially acute in space, where robots must operate on irregular regolith, spacecraft hulls, or asteroid surfaces without reliable infrastructure.

Nature offers a compelling alternative through geckos and jumping spiders, which achieve gravity-defying climbs via dry adhesion powered by van der Waals forces. These forces, arising from transient molecular interactions between nanoscale spatulae (flattened tips of gecko setae) and surfaces, enable strong, reversible attachment without energy expenditure [14–18]. The hierarchical microstructure of gecko feet composed of millions of branched setae and spatulae maximizes surface contact, distributing forces to prevent detachment while allowing rapid release via shear-induced peeling [19]. This mechanism has inspired synthetic adhesives that replicate gecko-like adhesion, such as elastomeric micropillars, carbon nanotube arrays, and directional fibrillar structures [20–32]. Unlike suction or magnets, gecko-inspired adhesives require no external power, function across diverse substrates (e.g., glass, metal, rough surfaces), and excel in environments where traditional methods fail such as vacuums or dusty conditions, making them ideal solutions for space robotics, planetary exploration, and terrestrial inspection tasks.

Despite these advancements, integrating dry adhesives into mobile climbing robots remains a formidable challenge. While some synthetic adhesives can sustain shear stresses of 10–20 kPa under laboratory conditions, their effectiveness declines on rough, irregular, or contaminated surfaces due to the lack of true nanoscale hierarchical compliance [10]. many climbing platforms, such as StickyBot and Abigaille-III, exhibit reliable performance on smooth vertical walls but falter during transitions across slopes, curved geometries, or discontinuities where contact angle and loading conditions vary unpredictably [33, 34]. This limitation is exacerbated by the underdeveloped coordination between adhesive engagement and leg motion. Stable climbing requires synchronized control that ensures

***Corresponding author:** Motaz Hassan, Department of Mechanical Engineering, The University of Akron and Department of Biomedical Engineering, The University of Akron, USA. Email: mmr93@uakron.edu

adhesion of sufficient legs during gait cycles, which is particularly important in low-gravity scenarios where gravitational loading does not naturally bias the robot toward the surface. Existing space-focused research, such as Hoang et al.'s work [35] on gecko-inspired orbital grippers, demonstrates promise in adhesion mechanics but does not yet address how to integrate these materials into complex, legged locomotion systems with dynamic surface interaction.

A persistent bottleneck for advancing climbing robots in space applications especially within academic settings is the limited availability of realistic and accessible microgravity testbeds. High-fidelity validation typically depends on infrastructure such as parabolic flights, neutral buoyancy labs, or drop towers, which are prohibitively expensive and often restricted to government or industrial partners [36–42]. To compensate, researchers often rely on low-cost analogs like helium balloon offloading or cable suspension systems, which introduce artificial constraints and fail to capture the inertial dynamics or unconstrained motion characteristic of true microgravity [43]. Recent works have developed reduced-gravity or lower gravity demonstratable testbeds using counterweights and degrees of freedom (DOF) motion tracking to emulate realistic planetary surfaces [44]. CBK-PAN's planar air-bearing platforms for robotic arm control under microgravity conditions serves as another illustrative system of offloading [45]. Both contain potential with drawbacks in balancing complexity, automation, and experimental fidelity. Compounding this is a significant gap in the literature regarding how climbing robots respond to non-discrete transitions between surface inclinations. Much of the current work evaluates locomotion only on horizontal or vertical planes, neglecting how performance shifts across continuously varying slopes [5, 46, 47]. This oversight masks critical behaviors related to adhesive loading, weight distribution, and gait stability during real-world traversal. In actual space scenarios, such as spacecraft hulls, planetary installations, or asteroid surfaces, robots must navigate compound angles, concavities, and curvature while coping with variable inertial forces. Addressing these dynamic interactions is essential for designing robust surface-mobile platforms capable of adaptive locomotion in low-gravity environments.

In this study, we propose a novel approach to bridge both material and infrastructure limitations. We present a directionally adhesive hexapod robot capable of controlled locomotion under a constrained two-degree-of-freedom (2-DOF) offloaded system, designed to emulate surface interaction in reduced gravity. Unlike full suspension rigs, this setup constrains the third axis while allowing horizontal and vertical motion, offering better control and more realistic locomotion than balloon-based or wired approaches. The hexapod employs a custom gecko-inspired adhesive pad cast from diffraction-grating materials (low-cost manufacturability) to passively engage and disengage through shear-based detachment. Drawing on insect-inspired gait patterns, the robot maintains a minimum of three legs in contact with the surface, maximizing stability during motion. The system also leverages a scalable, lithography-free adhesive manufacturing method, enabling rapid prototyping for constrained environments such as low Earth orbit (LEO). By uniting advances in synthetic adhesion with a controllable, low-cost experimental platform, this work contributes to the growing field of surface-mobile space robotics and addresses a critical gap in academic microgravity emulation for robotic adhesion studies.

2. Materials and Methods

2.1. Robotic design

The robot designed for this study is a hexapod, equipped with six articulated legs, each possessing two DOF: one for swinging the hip and the other for lifting the foot off the ground. This design builds upon our previously published model, which details the forward and inverse kinematics formulations for each joint, enabling precise control of leg trajectories during locomotion [48]. The body is constructed from polylactic acid (PLA) to reduce weight while maintaining the necessary structural integrity for climbing tasks. Central to the robot's operation is a Raspberry Pi microcontroller, which coordinates the actions of the legs through the use of 12 servos, 6 for controlling the hip movement and 6 for controlling the movement of the feet. The servos are driven by pulse width modulation (PWM) signals, which were calibrated through a custom-written python script. The calibration process involved determining the neutral position of each servo, the high (forward) position, and the low (backward) position, which provided the necessary range of motion for the robot's gait. The foot structure is critical for the robot's ability to climb vertical surfaces. In this robot, the feet were equipped with gecko-inspired adhesive pads with a micro-structured pattern designed to maximize surface contact and enhance adhesion. These pads worked in conjunction with the robot's gait, ensuring stable attachment while at least three feet remain in contact with the surface at any given time. The foot design was engineered for flexibility, allowing it to adapt to the surface profile while maintaining stable adhesion. Each foot was lifted in a controlled vertical motion, repositioned to maintain stable attachment, and then dropped back onto the surface using the passive system. This gait ensured that the robot progresses forward while retaining effective attachment through the gecko-inspired adhesive system.

Figure 1(a) presents a CAD model of a six-legged geckoinspired climbing robot designed for directional adhesion and modular locomotion, while Figure 1(b) presents each leg is independently actuated and equipped with footpads intended for shear-based contact with surfaces.

Figure 1
CAD representation of the proposed robotic configuration with its unique foot design

(a)

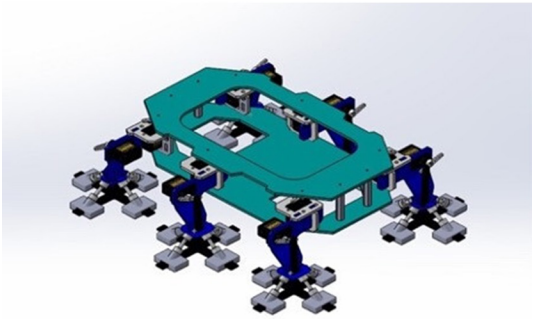

(b)

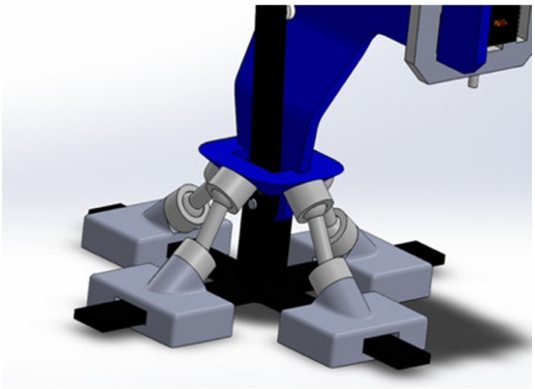

Once the servos were calibrated, the custom gait algorithm allowed precise control of the robot's movements, enabling the creation

of a forward-moving gait. The primary objective was to ensure that the robot could lift three legs at a time while maintaining at least three feet in contact with the surface to ensure stability. This sequential movement allows for the robot to propel itself forward while maintaining the necessary attachment to the surface via gecko-inspired adhesive. Each foot of the robot was designed with a passive element of movement that allowed the foot to lift and drop with minimal energy input. The passive movement was facilitated by a ball and socket joint mechanism embedded within each foot. The mechanism allowed the foot to naturally disengage through movement in the opposite shear direction from the surface during the lifting phase while providing controlled re-engagement when the foot dropped back onto the surface. This passive system reduced the energy and weight expenditure required to lift and position the feet, contributing to the overall energy efficiency of the robot's gait.

To enhance adaptability during unexpected terrain transitions or slippage events, the robot was equipped with an MPU-6050, an onboard Inertial Mesurement United (IMU), which continuously monitors body orientation and acceleration vectors similar to our previous study by Hassan et al. [48]. When deviations from expected locomotion patterns were detected such as during partial loss of adhesion or unbalanced shear loading, the control system dynamically adjusted the gait by slowing movement and increasing the number of legs simultaneously in contact with the surface. This reactive modulation compensated for reduced adhesive performance on sloped or uneven substrates and mimics terrain-aware behaviors seen in biological climbers. By integrating real-time proprioceptive sensing with adaptive gait control, the robot demonstrated the capacity to maintain mobility and stability in conditions where purely open-loop strategies would fail. This capability is essential for climbing in complex environments such as spacecraft exteriors, where gravitational cues, inertial forces, and surface angles vary continuously.

2.2. Gecko-inspired adhesive fabrication

The gecko-inspired adhesive system developed for this robotic platform incorporated a diffraction-grated pattern engineered to replicate the hierarchical microstructures found on gecko and anole toe pads. This design leveraged van der Waals forces generated by microscale surface features that maximize contact area, enabling strong yet reversible adhesion without chemical bonding. The pattern enhanced both shear and normal adhesion, supporting locomotion on vertical and inverted surfaces. Fabrication of the adhesive utilized a low-cost, cleanroom-free process involving soft lithography [49]. A master mold with a 7 µm groove spacing was fabricated via precision diamond ruling by a commercial supplier, providing a high-resolution pattern suitable for microscale replication. PDMS (RTV silicone in a 10:1 ratio), selected for its flexibility, aerospace compatibility, and low surface energy, was cast onto the mold to replicate the directional microgrooves. Scanning electron microscopy (Figure 2(a)) confirmed accurate replication of the intended periodicity, demonstrating consistent microgroove formation critical for directional dry adhesion. Once cured, the PDMS surface exhibited wedge-shaped ridges that balance compliance and adhesion. The adhesive was integrated into the robot's feet with its orientation aligned for optimal shear resistance; sliding in the reverse direction disengages the contact passively. Importantly, this approach eliminates the need for nanoscale fabrication or cleanroom facilities, offering rapid, scalable, and low-cost production. In an unpublished experimental study, this adhesive achieved a peak shear strength of 7.78 kPa over a contact area of 103.23 cm², validating its mechanical performance and suitability for both terrestrial and space applications.

Figure 2 is produced in BioRender.com. Figure 2(a) presents SEM image of the patterned adhesive surface replicated from a master mold with 15 µm periodicity, produced via precision diamond ruling. The micro-ridged grooves are visibly aligned and uniform, providing directional surface anisotropy critical for controlled adhesion. Figure 2(b) presents a schematic representation of the fabrication process, from mold preparation to PDMS casting, curing, and demolding. Both sections are used in our recent study [49].

Figure 2
SEM of the patterned adhesive surface replicated from a master mold along with the microfabrication process to develop the gecko-inspired adhesive

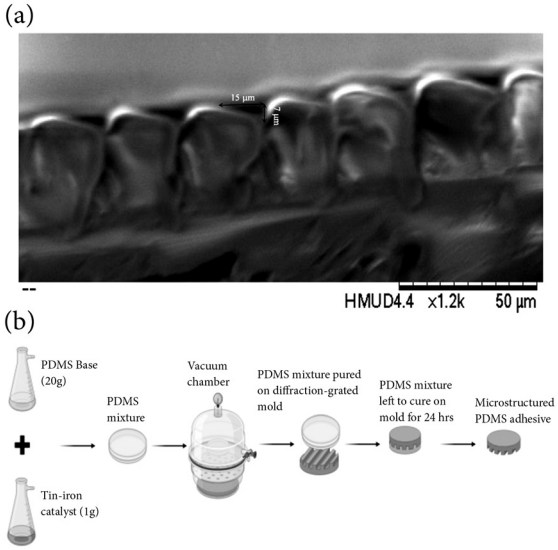

2.3. Manual offloading system for robotic locomotion experiments

To emulate reduced-gravity conditions without the high cost or infrastructure of aerospace-grade facilities, a custom offloading system was designed, drawing inspiration from NASA's reduced-gravity test platforms. This system relies on a tension-based suspension mechanism guided by the robot's center of mass (CoM), which was precisely calculated using SolidWorks. A CAD representation of the robot assembly (Figure 3), including SolidWorks-determined CoM, was used to identify optimal lift points for offloading both vertically and horizontally. This setup was manually operated, which could introduce some variability; it provides a flexible, low-cost platform to explore locomotion trends across multiple inclinations and robot configurations.

SolidWorks CAD renderings of the quadruped Figure 3(a) and hexapod Figure 3(b) robot configurations with the calculated CoM visualized as a blue and white marker. The CoM was used to inform vertical and horizontal offloading positions during reduced-gravity testing. Symmetrical servo placement and internal electronics influence the CoM location, which serves as the basis for load distribution through the offloading suspension system.

The robot was suspended using multiple tensioned lines attached to its chassis at carefully selected locations, ensuring that the force distribution aligned with the CoM to avoid rotational imbalances (Figure 4). These lines converged at a central tether routed through a roller-based overhead gantry. This setup permitted the robot to remain suspended with minimal friction, allowing near-planar movement while maintaining structural equilibrium. The gantry system was coupled with a 91.44 cm × 91.44 cm × 0.2032 cm (length × width × thickness) acrylic test platform, mounted on an adjustable tilting frame that allows surface inclinations of 0°, 5°, 10°, 15°, 30°, 45°, 60°, and 90°. To counteract unintended torques or lateral drift during operation, side constraints are incorporated to stabilize the robot during vertical

and inclined locomotion. Future iterations of the system aim to explore semi-automated or counterweighted offloading to reduce operator-dependent variability and enhance reproducibility.

Figure 3
SolidWorks schematics with the center of mass highlighted per robotic configuration

(a)

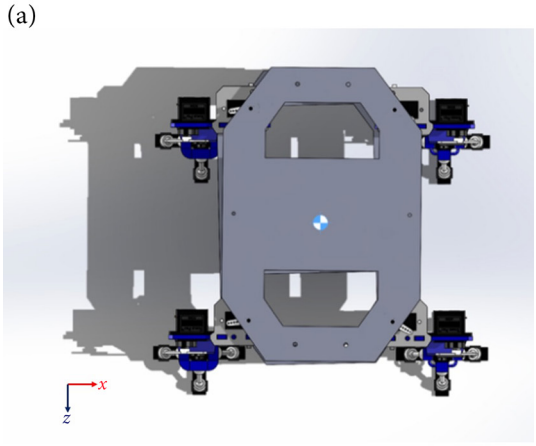

(b)

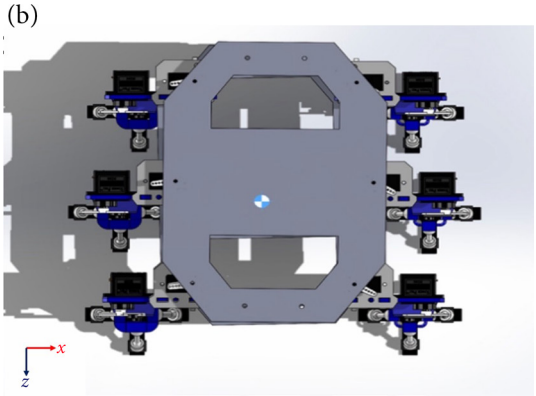

Figure 4
The experimental offloading fixture and design

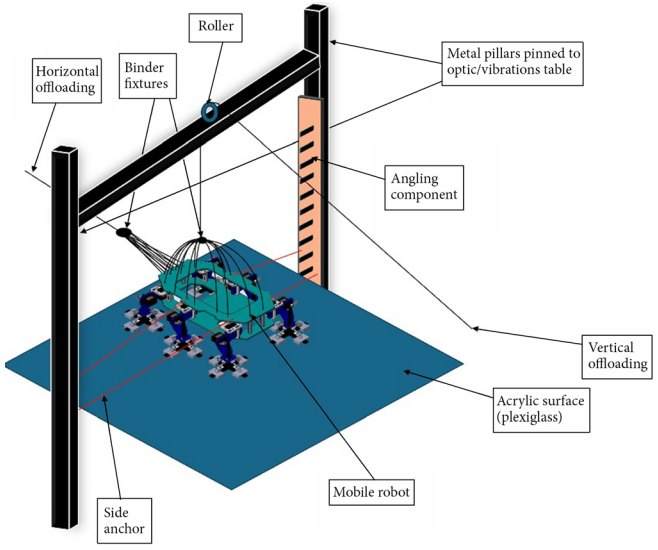

An experimental offloading system was designed to simulate reduced-gravity conditions for a gecko-inspired climbing robot. The setup included vertical and horizontal offloading via binder fixtures and a roller, which allowed the robot to operate on a vertical acrylic surface while experiencing near-weightless conditions. Metal pillars and a side anchor were used to maintain structural stability, and the angling component adjusted the slope for variable testing scenarios.

Two principal force vectors governed the offloading manipulation. In the x and y directions (parallel to the incline and perpendicular to the incline, respectively), the force required to simulate reduced weight was determined using the decomposition of gravitational force in a 2D capacity, as shown in Equations (1) and (2):

$$F_x = mg\cos(\theta) \tag{1}$$

$$F_y = mg\sin(\theta) \tag{2}$$

where m is the total mass of the robot, g is the acceleration due to gravity, and θ is the angle of inclination of the test surface. The offloading process was manually controlled: one operator pulled tangentially in the intended direction of locomotion, while another applied a stabilizing force perpendicular to the surface to counteract undesired motion. This experimental framework supports locomotion analysis for multiple robotic configurations, including four-legged and six-legged versions, each tested with and without gecko-inspired adhesive pads. Each trial was conducted under two conditions: standard gravity and reduced gravity using the offloading system. Key performance metrics wer etotal displacement (cm), trial duration (s), and cycle slip (cm), representing unintended backward motion per step. From these, velocity (cm/s) and movement efficiency (ratio of effective forward displacement to total movement) were calculated to assess the robot's climbing performance. While the current adhesive characterization is limited, these experiments serve as initial functional validation; systematic adhesion testing under multiple surfaces and load conditions is ongoing.

Vertical climbing and inclined surface trials evaluate how adhesive engagement and leg design influence stability. The six-legged configuration, which offers a higher number of contact points and broader surface area for adhesion, is hypothesized to improve load distribution and traction under reduced-gravity conditions. Comparative analysis across these configurations provides insight into the role of mechanical support geometry in adhesion-enabled robotic locomotion.

To quantify the variability inherent in the manually operated reduced-gravity simulation, each locomotion trial was repeated multiple times and all key metrics were reported as mean ± standard deviation (SD). The SD captured the variability introduced by manual offloading forces in both tangential and perpendicular directions, as well as minor differences in adhesive engagement during locomotion. This approach provides a measure of reproducibility for the experimental platform and allows for assessment of performance trends despite operator-induced variability. While a semi-automated or counterweighted system may reduce this variability in future work, the current SD values demonstrate that the manually operated gantry provides sufficiently consistent conditions to evaluate robot locomotion across different surface inclinations and adhesive configurations.

3. Results

To assess the performance of the mobile robot's adhesive system, initial trials were conducted under full gravity conditions on the acrylic surface. The robot was tested in two configurations: with adhesion disabled and with adhesion enabled. Figure 5 illustrates the robots under these experimental conditions. Figure 6 shows the total distance travelled of the robot with and without adhesion without offloading.

Climbing performance of the mobile robot platforms under varying gravity conditions: The six-legged robot tested under offloaded (reduced gravity) conditions climbs a vertical 90° surface (Figure 5(a)). The four-legged configuration, operating under full gravitational load,

demonstrates stable adhesion-assisted locomotion at a 45° incline (Figure 5(b)).

Figure 5

Both robotic configurations traversing the experimental apparatus

(a)

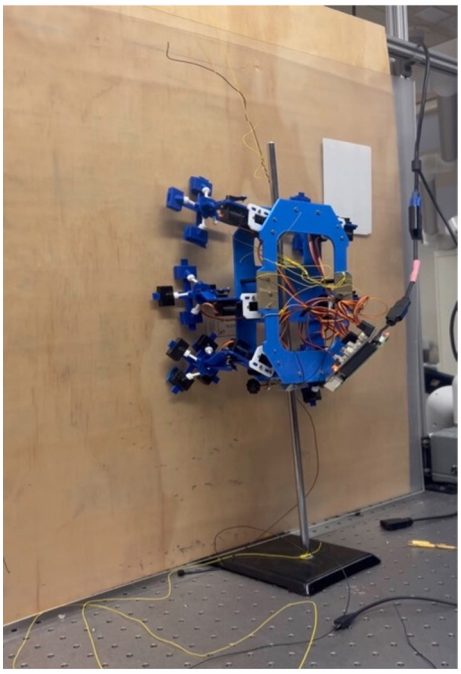

(b)

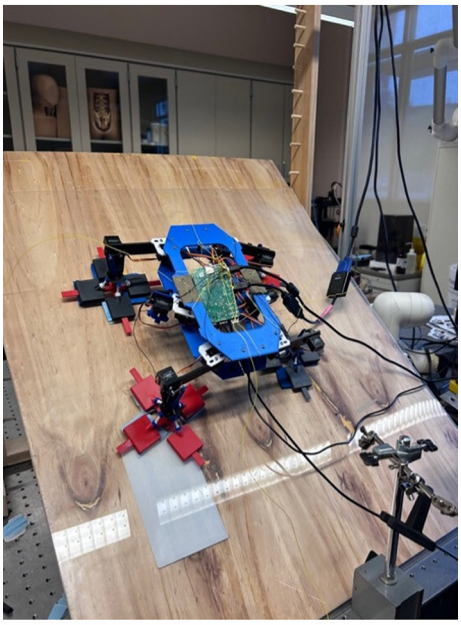

To evaluate how adhesion and slip angle affect locomotion performance, both four-legged and six-legged robots were tested under varying surface conditions. Robots were operated with and without adhesive pads, and their movements were analyzed at slip angles of 0°, 5°, and 10°, simulating stable and inclined surface scenarios. Performance metrics included total movement, forward and backward displacement, velocity, and a calculated adhesion efficiency, which quantifies the robot's ability to translate motion forward while minimizing slippage. The results are summarized in Table 1. All locomotion metrics are reported as mean ± SD to capture variability introduced by manual offloading forces and minor variations in adhesive engagement. These SD values provide a quantitative measure of reproducibility across trials, showing that despite operator-induced variability, trends in displacement, velocity, and efficiency are consistent.

Figure 6

Average total movement across slip angles for both robotic configurations

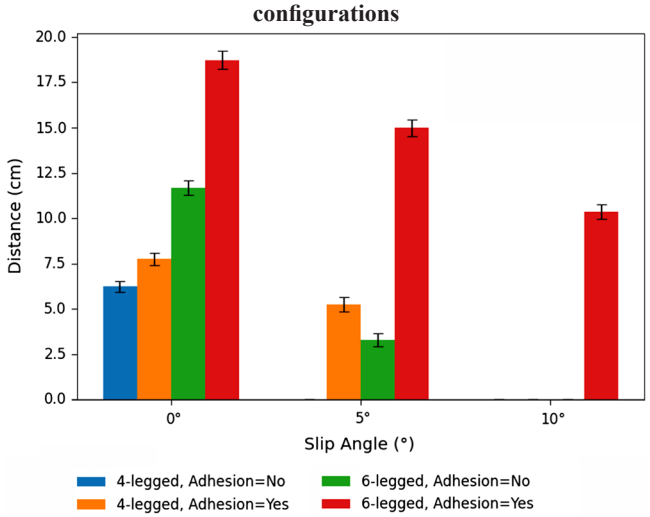

Note: Average total movement (mean ± SD) of 4-legged and 6-legged robot configurations with and without adhesive under varying slip angles (0°, 5°, and 10°). Error bars indicate standard deviations.

For both four-legged and six-legged robots, the use of adhesion at 0° slip angle substantially increased forward displacement while minimizing or eliminating backward drift, leading to a calculated adhesion efficiency of 100.0 ± 0.0%. Without adhesion, the four-legged robot showed minimal forward movement (0.75 ± 0.1 cm) and very low velocity (0.22 ± 0.05 cm/s), while the six-legged robot, despite achieving a higher total movement, displayed negligible net progress, suggesting inefficiencies due to leg slippage and potential in-place gaiting. As slip angle increased to 5°, the four-legged robot with adhesion demonstrated a sharp decline in forward progress (0.56 ± 0.1 cm) and an introduction of backward movement (0.63 ± 0.08 cm), reducing its adhesion efficiency to 69.1 ± 4.5%. In contrast, the six-legged robot maintained a higher forward displacement (2.91 ± 0.15 cm) and velocity (2.91 ± 0.12 cm/s) under the same conditions, though its efficiency also dropped to 53.7 ± 5.0%, indicating partial losses due to slipping. At 10° slip, the six-legged robot experienced a further decline in forward movement (2.17 ± 0.25 cm) and a significant increase in backward slippage (3.72 ± 0.25 cm), bringing adhesion efficiency down to just 41.6 ± 4.0%. Variability was greatest at these higher inclines, reflecting the sensitivity of adhesion to slip angle and manual offloading forces. Overall, the six-legged robot consistently outperformed the four-legged robot in adaptability and net displacement, likely due to its ability to distribute load more evenly across additional limbs. However, the results also highlight that beyond a certain slip threshold, efficiency loss becomes unavoidable as slippage overcomes adhesive strength.

Following the inclined surface trials, tests were conducted to evaluate the robots' performance during offloading maneuvers. These tests (Table 2) were performed with both horizontal and vertical orientations to simulate detachment and repositioning scenarios. The measured metrics were similar to the original experiment; however, stationary adhesion was included to indicate how the robots operate when placed on the acrylic surface at given angles without movement. The offloading trials (Table 2) demonstrated the ability of the manual 2-DOF gantry system to reproduce reduced-gravity conditions across

a range of inclines. While operator-controlled offloading introduces variability, the consistent trends in movement metrics and SD values indicate that the platform provides a reproducible and representative approximation of partial gravity for evaluating adhesive-enabled locomotion.

Offloading performance metrics for four-legged and six-legged robots across varying incline angles (slip). Tests evaluated displacement, velocity, duration, slip, and adhesion efficiency during horizontal and vertical detachment simulations. Results show a decline in movement efficiency and stationary adhesion with increasing incline, with the six-legged robot generally outperforming the four-legged configuration across most parameters.

The results detail the offloading performance of both the four-legged and six-legged robots under simulated gravity conditions, represented by varying offloading force components F_x and F_y, which correspond to the resolved gravitational vectors along and perpendicular to the test surface, respectively. As the slip angle increased from 0° to 90°, F_y progressively increased, while F_x decreased, simulating a transition from horizontal to vertical loading. This shift significantly impacted locomotion performance across both robotic configurations. A clear decline in total movement, velocity, and movement efficiency was observed with increasing inclination, though the SD values (e.g., 20.97 ± 0.65 cm total displacement for the six-legged robot at 0°) confirm reproducibility across trials. The six-legged robot consistently outperformed the four-legged version in total displacement (20.97 ± 0.65 cm vs. 13.98 ± 0.35 cm at 0°), velocity (0.69 ± 0.08 cm/s vs. 0.46 ± 0.06 cm/s), and movement efficiency, particularly at higher inclines. At 5° slip, the six-legged robot retained 98.3 ± 2.0% efficiency versus 95.0 ± 2.0% in the four-legged version, with the performance gap widening as the incline increased. By 45°, the four-legged robot dropped to 29.9 ± 7.0% efficiency and could no longer maintain stationary adhesion, while the six-legged robot sustained 76.4 ± 6.0% efficiency and adhered reliably.

Beyond 45°, both robots began losing adhesion, but the six-legged configuration continued to exhibit superior resilience, maintaining 67.3 ± 7.0% efficiency at 60° and 56.3 ± 8.0% even at the extreme vertical (90°) scenario compared to just 2.0 ± 1.0% and 0%, respectively, for the four-legged version. These outcomes show

Table 1
Impact of adhesion and slip angle on locomotion performance of four-legged vs. six-legged robot under full gravity conditions

Robot type	Adhesive Added	Slip (°)	Average Total movement (cm)	Average Duration (s)	Average Velocity (cm/s)	Average Forward movement (cm)	Average Backward movement (cm)	Average Movement efficiency (%)
4-legged	No	0	6.24 ± 0.3	28.45 ± 0.5	0.22 ± 0.05	0.75 ± 0.1	0.00 ± 0.0	100 ± 0.0
	Yes	0	7.75 ± 0.35	28.49 ± 0.5	0.27 ± 0.06	1.17 ± 0.15	0.00 ± 0.0	100 ± 0.0
	Yes	5	5.25 ± 0.4	28.36 ± 0.6	0.19 ± 0.05	0.56 ± 0.1	0.63 ± 0.1	12.50 ± 2.0
6-legged	No	0	11.68 ± 0.4	30.73 ± 0.6	0.38 ± 0.08	0.38 ± 0.1	0.00 ± 0.0	100 ± 0.0
	No	5	3.30 ± 0.35	30.68 ± 0.7	0.21 ± 0.06	0.21 ± 0.1	0.84 ± 0.15	6.44 ± 1.5
	Yes	0	18.72 ± 0.5	30.73 ± 0.6	2.91 ± 0.12	2.91 ± 0.15	0.00 ± 0.0	100 ± 0.0
	Yes	5	14.99 ± 0.45	30.52 ± 0.7	2.16 ± 0.15	2.16 ± 0.2	0.95 ± 0.15	56.10 ± 5.0
	Yes	10	10.38 ± 0.4	30.30 ± 0.6	2.17 ± 0.12	2.17 ± 0.25	3.72 ± 0.2	41.60 ± 4.0

Table 2
Impact of offloading on robotic configurations and their ability to adhere to an acrylic surface

Robot type	Slip (°)	F_x (N)	F_y (N)	Average Total Movement (cm)	Average Duration (s)	Average Velocity (cm/s)	Average Slip (cm)	Average Movement Efficiency (%)	Stationary Adhesion
4-legged	0	8.59 ± 0.15	0 ± 0.0	13.98 ± 0.3	30.73 ± 0.5	0.46 ± 0.05	0.00 ± 0.0	100 ± 0.0	Yes
	5	8.55 ± 0.2	0.75 ± 0.1	14.23 ± 0.35	30.52 ± 0.6	0.47 ± 0.05	0.71 ± 0.1	95.01 ± 2.0	Yes
	10	8.46 ± 0.25	1.49 ± 0.15	11.34 ± 0.4	30.30 ± 0.6	0.37 ± 0.06	2.74 ± 0.2	75.84 ± 4.0	Yes
	15	8.30 ± 0.3	2.22 ± 0.2	10.50 ± 0.45	30.68 ± 0.7	0.34 ± 0.07	3.58 ± 0.25	65.90 ± 5.0	Yes
	30	7.44 ± 0.35	4.29 ± 0.3	9.89 ± 0.5	30.73 ± 0.75	0.32 ± 0.08	4.23 ± 0.3	57.23 ± 6.0	Yes
	45	6.07 ± 0.4	6.07 ± 0.35	8.23 ± 0.55	30.54 ± 0.8	0.27 ± 0.09	5.82 ± 0.35	29.98 ± 7.0	No
	60	4.29 ± 0.45	7.44 ± 0.4	7.48 ± 0.6	30.68 ± 0.85	0.24 ± 0.1	7.33 ± 0.4	2.01 ± 1.0	No
	90	0.00 ± 0.5	8.59 ± 0.45	6.74 ± 0.65	30.54 ± 0.9	0.22 ± 0.11	8.84 ± 0.5	0 ± 0.0	No
6-legged	0	8.59 ± 0.15	0.00 ± 0.0	20.97 ± 0.4	30.73 ± 0.5	0.69 ± 0.06	0 ± 0.0	100 ± 0.0	Yes
	5	8.55 ± 0.2	0.75 ± 0.1	21.35 ± 0.45	30.52 ± 0.6	0.71 ± 0.07	0.36 ± 0.05	98.31 ± 2.0	Yes
	10	8.46 ± 0.25	1.49 ± 0.15	17.01 ± 0.5	30.3 ± 0.65	0.56 ± 0.08	1.37 ± 0.1	91.95 ± 3.0	Yes
	15	8.30 ± 0.3	2.22 ± 0.2	15.75 ± 0.55	30.68 ± 0.7	0.51 ± 0.09	1.79 ± 0.15	88.63 ± 4.0	Yes
	30	7.44 ± 0.35	4.29 ± 0.3	14.84 ± 0.6	30.73 ± 0.75	0.48 ± 0.1	2.12 ± 0.2	85.71 ± 5.0	Yes
	45	6.07 ± 0.4	6.07 ± 0.35	12.35 ± 0.65	30.54 ± 0.8	0.41 ± 0.11	2.91 ± 0.25	76.44 ± 6.0	Yes
	60	4.29 ± 0.45	7.44 ± 0.4	11.22 ± 0.7	30.68 ± 0.85	0.37 ± 0.12	3.67 ± 0.3	67.29 ± 7.0	No
	90	0 ± 0.0	8.59 ± 0.45	10.11 ± 0.75	30.54 ± 0.9	0.33 ± 0.13	4.42 ± 0.35	56.28 ± 8.0	No

that the six-legged configuration consistently achieves a higher forward displacement, velocity, and movement efficiency across inclines, as measured by total displacement, velocity, and adhesion efficiency metrics. Notably, the six-legged robot was able to maintain stationary adhesion up to 45°, while the four-legged version lost this capability after 30°. Overall, the results confirm that gecko-inspired adhesion, when coupled with a robust multi-legged gait, offers significant advantages in traversing inclined or gravity-altered environments relevant to on-orbit servicing, planetary mobility, and vertical surface operations in space applications. Furthermore, the offloading system, though not designed for orbital mechanics, successfully achieved its intended role: producing controllable and repeatable reductions in effective weight, thereby validating its use as a ground-based testbed for partial-gravity locomotion studies.

4. Discussion and Outlook

4.1. Mechanical and design constraints

The robot's locomotion was shaped by its six-legged configuration, designed to optimize balance and maintain continuous contact with the climbing surface. While this provided enhanced stability over earlier four-legged prototypes, it introduced a higher burden on coordination and timing. Each leg had two DOF, enabling forward swing and vertical lift. However, the absence of compliance in the leg structure and the rigidity of the PLA frame limited the robot's ability to conform to curved or uneven surfaces. As a result, full adhesive contact was only achieved when foot placement and gait timing were precisely aligned. These mechanical constraints significantly affected the robot's ability to maintain adhesion, especially during rapid movements or at steeper inclines. Furthermore, because the system relied on open-loop control with predefined trajectories, it lacked the capability to correct minor deviations in foot orientation or surface irregularities during locomotion. Small perturbations in gait resulted in significant reductions in adhesive contact area and, in turn, locomotion performance. For instance, at 10° slip, forward displacement dropped to just 2.17 ± 0.25 cm while backward slippage reached 3.72 ± 0.25 cm, reducing efficiency to 41.6 ± 4.0%. These values underscore how even modest geometric misalignments can lead to steep performance losses. These findings highlight the perilous need for future integration of compliant elements and real-time feedback control to allow micro-adjustments during climbing, particularly in environments where perfect surface alignment cannot be guaranteed.

Incorporating flexible materials or tendon-driven actuators within each leg could allow the robot to dynamically adapt its foot placement in response to contact conditions [50]. Adding proprioceptive sensing at the foot or joint levels such as force-sensitive resistors or miniature torque sensors would enable the system to detect improper foot engagement and adjust its gait trajectory in real time [51–54]. This approach would bridge the current gap between open-loop design simplicity and the need for complex, surface-conforming control in variable environments.

4.2. Adhesion and detachment mechanics

While the fabricated gecko-inspired adhesive demonstrated strong performance under controlled shear, one of the most significant barriers to continuous locomotion was effective detachment. Natural geckos use a peeling mechanism, starting at one edge of the toe pad and rolling the contact area off the surface in a controlled manner [55]. In contrast, the robot's design featured a passive ball-joint at the foot, which allowed some angular motion but provided no active assistance in peeling. This led to situations where feet remained partially adhered during the lift phase, requiring excess energy from the servos to complete detachment especially problematic when the robot was operating on inclines. The lack of an integrated detachment mechanism resulted in disrupted gait patterns, occasional foot drag, and even momentary immobilization, particularly at shear angles above 10°. At higher slip angles, this manifested as reduced gait repeatability, with efficiency falling from 53.7 ± 5.0% at 5° to just 41.6 ± 4.0% at 10°. These trends show that detachment mechanics were equally limiting as adhesion strength. These instances affected not only energy efficiency but also increased wear on both the adhesive and the servos. Detachment timing proved to be as critical as adhesion strength for ensuring uninterrupted locomotion.

To address this limitation, future iterations should incorporate spring-loaded toe peeling mechanisms or shape-memory actuation that initiates detachment through an edge-peel motion [5, 56–58]. Such systems could enable directional release of adhesion with minimal torque requirements. For instance, a simple compression spring embedded in the toe joint could initiate toe lifting once servo motion ceases, reducing energy usage and detachment time. Alternatively, electro-adhesion or thermally activated release layers could be explored to allow active control over the adhesive state [13, 59–62]. The broader implication is that adhesion must not only be strong, but it must also be controllable. Mechanical detachment is central to achieving gait repeatability and system longevity, particularly for mission-critical climbing operations in space.

4.3. Foot design and adhesive interface

The design of the robot's foot played a central role in its ability to engage and release from vertical surfaces. Each footpad was designed to be flat and slightly compliant to match the planar substrate. However, the robot's lack of fine toe articulation reduced the ability of the footpad to adapt to micro-topographical variations on the climbing surface. Adhesion was maximized only when the pad was pressed uniformly and nearly perpendicular to the surface. Even slight angular misalignments, common during inclined or unbalanced stances, reduced the contact area and weakened adhesion, leading to early detachment or foot slip. This was particularly evident in trials without adhesion, where the four-legged robot managed only 0.75 ± 0.1 cm of forward displacement at 0° despite 6.24 ± 0.3 cm of total movement, reflecting ~88% of effort lost to slippage. Additionally, the row-based adhesive structure, while robust and durable under moderate loads, was not optimized for contact redundancy. If a section of the foot did not make contact, the robot had no mechanism to redistribute load or conform the pad dynamically. This limitation was quantified by larger standard deviations at higher inclines, where variability in adhesive contact dominated trial-to-trial outcomes. This revealed the importance of foot-level compliance and multi-zone engagement, both hallmarks of biological gecko systems. These characteristics enable the animal to maintain adhesion over rough or curved terrain with minimal control effort.

Improvements to the foot structure could include a hierarchical or segmented toe layout, allowing multiple smaller adhesive zones to operate independently [63]. Soft robotics approaches such as embedding pneumatic channels or low-durometer silicone layers could also enhance surface compliance [64, 65]. Furthermore, embedding tilt sensors or using a camera-based toe-alignment system could allow the robot to assess its contact geometry before committing to a step. The development of a modular foot architecture would also allow the robot to adapt its foot morphology based on surface type, incline, or application, increasing mission versatility.

4.4. Gait performance and stability

The six-legged configuration afforded the robot a more robust and fault-tolerant gait, particularly when traversing inclined

surfaces. This was especially evident during trials using the gecko-inspired adhesive, where increased surface engagement translated to improved slip resistance and forward progression [56, 66]. At 0° slip, the six-legged robot with adhesion achieved 18.72 ± 0.5 cm of forward displacement at 2.91 ± 0.12 cm/s, compared to only 11.68 ± 0.4 cm at 0.38 ± 0.08 cm/s without adhesion, a ~60% improvement. However, the increased number of legs also required more complex gait sequencing. Small synchronization errors led to overloading of certain legs, shifting the robot's center of mass and compromising balance. Additionally, due to the passive design of the ball-joint foot, slipping one leg could sometimes cause an entire side of the robot to shift or roll slightly, breaking uniform adhesion across other legs. This was reflected in offloading trials, where efficiency diverged sharply between robot types: at 90° reduced gravity, the hexapod retained 56.3 ± 8.0% efficiency, while the quadruped dropped to 0%. This sensitivity to gait timing and center-of-mass shifts suggests that beyond adhesion, gait mechanics must be tightly coupled with force distribution and foot placement accuracy [67].

The increased number of legs also increased the computational and mechanical burden of achieving synchronized motion, especially under variable incline or load conditions. Closed-loop gait control using inertial measurement units (IMUs) and footpad pressure sensors could allow the robot to monitor ground reaction forces in real time and adjust stride length or stance duration dynamically. Coupling this with adaptive gait planning algorithms such as central pattern generators (CPGs) with feedback modulation could allow for smooth and responsive gait adjustments on the fly [68–70]. Bioinspired gait strategies observed in insects and geckos including the alternating tripod gait for rapid progression, metachronal wave gait for stability on vertical planes, and ripple gaits for uneven terrain provide models for how adhesive climbing robots could balance speed, efficiency, and reliability depending on environmental demands [71, 72]. In the long term, the robot could adopt these bioinspired gaits based on environmental sensing, such as shifting from a tripod gait to a wave gait when climbing vertical surfaces, improving both energy efficiency and movement precision. By situating our findings alongside this body of gait optimization research, the present work highlights not only the importance of adhesives for slip resistance but also the need for integrated gait–adhesion strategies to achieve reliable climbing under reduced-gravity conditions.

4.5. Experimental gantry system and future improvements

The custom 2-DOF gantry system developed for this study provided a cost-effective method to emulate reduced gravity by decomposing gravitational forces into tangential and normal components. This setup enabled planar locomotion tests at inclinations ranging from 0° to 90°, allowing systematic evaluation of adhesion-enabled climbing under partial weight support. The reproducibility of the platform was reflected in relatively low variability at shallow inclines (e.g., 20.97 ± 0.65 cm displacement at 0° for the six-legged robot), confirming that the system is sufficient for identifying locomotion trends. However, manual offloading introduced variability in higher-slip trials, where operator force fluctuations caused larger standard deviations. At steeper inclines, this variability partially obscured adhesive and gait contributions, limiting the precision of quantitative comparisons across conditions. Another limitation is that the current gantry constrains motion to a planar surface and does not account for inertial dynamics such as rotational drift, angular momentum, or free-fall trajectories characteristic of true microgravity. Expanding the system to include additional DOF would enhance this system. For instance, mounting the testbed on air bearings, spherical gimbals, or omnidirectional suspensions would allow more realistic simulation of body tumbling, surface reorientation, and six-DOF motion. These capabilities are critical for testing adhesion robustness during transitions across compound geometries, curved spacecraft hulls, or asteroid surfaces where inertial effects dominate.

Automation offers a path to address these shortcomings. Incorporating counterweights, linear actuators, or motorized winches integrated with load cells could apply constant, closed-loop controlled offloading forces aligned with the robot's center of mass. Such a system would eliminate operator-induced noise and maintain force vector accuracy throughout trials. Furthermore, multi-axis force sensing could ensure that vertical and horizontal components are modulated dynamically as the robot transitions across slopes, replicating the continuously varying gravitational vectors encountered in real environments. By automating load application and expanding the degrees of freedom available in the offloading mechanism, the gantry could evolve into a higher-fidelity partial-gravity emulator. Such an approach would bridge the gap between benchtop testing and costly infrastructure such as parabolic flights or neutral buoyancy labs, providing the academic community with a scalable platform to study adhesive-enabled locomotion under conditions that more closely approximate microgravity.

4.6. Broader implications and future applications

While this project was focused on validating a gecko-inspired climbing robot using custom-fabricated adhesives, the broader goal was to assess the feasibility of such systems for applications in constrained, unpredictable, or zero-gravity environments. The success of the robot under partial gravity and inclined testing conditions demonstrates that adhesive-based locomotion can be translated into engineered systems with predictable, directional adhesion. The numerical performance trends observed, ~60% displacement gains at 0° slip, but <42% efficiency at 10° slip, illustrate both the promise and limits of current dry adhesive integration. The implications for in-orbit servicing, inspection, and planetary exploration are substantial, particularly as surface access becomes more critical for satellite repair and infrastructure maintenance. However, this study also made clear that adhesion alone is insufficient. Without reliable detachment, adaptive gait control, and compliant foot mechanisms, the performance envelope of adhesive robots remains limited. Thus, space-relevant climbing robots must be designed as integrated adhesion–gait systems rather than adhesive platforms alone. Future space applications will demand robots that can operate autonomously over extended periods, adjust to unexpected surface geometries, and tolerate partial system failure without complete locomotion breakdown.

The next phase of development should focus on testing the system under high-fidelity microgravity simulations or aboard parabolic flights, where inertial effects and detachment behaviors can be more realistically observed. Additionally, integration with robotic arms or modular payloads could allow the climbing platform to double as a mobile manipulator for tool delivery or environmental sensing. There is also strong potential to scale the adhesive mechanism across robot size classes from centimeter-scale explorers to meter-scale mobile inspectors depending on application needs [73, 74]. Through a combination of mechanical innovation, biological inspiration, and systems-level integration, adhesive-based locomotion has the potential to reshape how mobile robots engage with surfaces in extreme environments.

5. Conclusions

This study demonstrated the feasibility of a six-legged robot employing a low-cost gecko-inspired adhesive system to achieve vertical locomotion on smooth surfaces. The robot's 2-DOF per leg allowed directional movement and foot lift, while the fabricated PDMS-based adhesive enabled controlled shear engagement. Experimental

results confirmed that stable locomotion is achievable when gait timing, surface contact, and adhesion mechanics are properly aligned. Quantitatively, adhesion increased displacement by up to ~60% at 0° slip (18.72 ± 0.5 cm vs. 11.68 ± 0.4 cm), while under reduced gravity the robot sustained 56.3 ± 8.0% efficiency at 90°, compared to 0% for the quadruped. Conversely, efficiency fell below 42% at 10° slip, revealing slippage as a dominant limitation. However, challenges arose in detachment consistency, gait synchronization, and foot conformity, highlighting critical limitations in mechanical design and control strategy. Overall, the work validates that directional adhesion can be integrated into legged robotic systems for surface climbing. Future development will focus on (1) compliant, segmented footpads for improved conformity; (2) active peeling mechanisms to reduce servo strain; and (3) closed-loop gait control for adaptive locomotion, all of which are essential to enable long-duration operations in space-relevant environments.

Ethical Statement

This study does not contain any studies with human or animal subjects performed by any of the authors.

Conflicts of Interest

The authors declare that they have no conflicts of interest to this work.

Data Availability Statement

Data are available from the corresponding author upon reasonable request.

Author Contribution Statement

Motaz Hassan: Methodology, Software, Validation, Formal analysis, Investigation, Resources, Data curation, Writing – original draft, Writing – review & editing, Visualization, Supervision, Project administration. **Oluwafemi Fayomi:** Methodology, Software, Validation, Formal analysis, Investigation, Resources, Data curation, Writing – original draft, Writing – review & editing, Visualization, Supervision, Project administration. **Joshua Faust:** Methodology, Software, Validation, Formal analysis, Investigation, Resources, Data curation, Writing – original draft, Writing – review & editing, Visualization. **Ajay Mahajan:** Methodology, Software, Formal analysis, Investigation, Resources, Writing – original draft, Writing – review & editing, Visualization.

References

[1] Alizadeh, M., & Zhu, Z. H. (2024). A comprehensive survey of space robotic manipulators for on-orbit servicing. *Frontiers in Robotics and AI*, *11*, 1470950. https://doi.org/10.3389/frobt.2024.1470950

[2] Hou, X., Su, Y., Jiang, S., Li, L., Chen, T., Sun, L., & Deng, Z. (2018). Adhesion mechanism of space-climbing robot based on discrete element and dynamics. *Advances in Mechanical Engineering*, *10*(4), 1687814018772934. https://doi.org/10.1177/1687814018772934

[3] Ren, Z. (2022). *Synthetic gecko inspired dry adhesive through two-photon polymerization for space applications*. Master's Thesis, Embry-Riddle Aeronautical University.

[4] Chen, T. G., Cauligi, A., Suresh, S. A., Pavone, M., & Cutkosky, M. R. (2022). Testing gecko-inspired adhesives with astrobee aboard the international space station: Readying the technology for space. *IEEE Robotics & Automation Magazine*, *29*(3), 24–33. https://doi.org/10.1109/MRA.2022.3175597

[5] Wang, B., Xiong, X., Duan, J., Wang, Z., & Dai, Z. (2021). Compliant detachment of wall-climbing robot unaffected by adhesion state. *Applied Sciences*, *11*(13), 5860. https://doi.org/10.3390/app11135860

[6] Bian, S., Wei, Y., Xu, F., & Kong, D. (2021). A four-legged wall-climbing robot with spines and miniature setae array inspired by longicorn and gecko. *Journal of Bionic Engineering*, *18*(2), 292–305. https://doi.org/10.1007/s42235-021-0032-0

[7] Gao, X., Yan, L., Wang, G., & Chen, I.-M. (2022). Modeling and analysis of magnetic adhesion module for wall-climbing robot. *IEEE Transactions on Instrumentation and Measurement,* 1–1. https://doi.org/10.1109/TIM.2022.3224522

[8] Sun, J., Bauman, L., Yu, L., & Zhao, B. (2023). Gecko-and-inchworm-inspired untethered soft robot for climbing on walls and ceilings. *Cell Reports Physical Science*, *4*(2), 101241. https://doi.org/10.1016/j.xcrp.2022.101241

[9] Tao, B., Gong, Z., & Ding, H. (2023). Climbing robots for manufacturing. *National Science Review*, *10*(5), nwad042. https://doi.org/10.1093/nsr%2Fnwad042

[10] Niewiarowski, P. H., Stark, A. Y., & Dhinojwala, A. (2016). Sticking to the story: Outstanding challenges in gecko-inspired adhesives. *Journal of Experimental Biology*, *219*(7), 912–919. https://doi.org/10.1242/jeb.080085

[11] Guo, J., Leng, J., & Rossiter, J. (2020). Electroadhesion technologies for robotics: A comprehensive review. *IEEE Transactions on Robotics*, *36*(2), 313–327. https://doi.org/10.1109/TRO.2019.2956869

[12] Alizadehyazdi, V., Modabberifar, M., Mahmoudzadeh Akherat, S. J., & Spenko, M. (2018). Electrostatic self-cleaning gecko-like adhesives. *Journal of The Royal Society Interface*, *15*(141), 20170714. https://doi.org/10.1098/rsif.2017.0714

[13] Alizadehyazdi, V., Bonthron, M., & Spenko, M. (2020). An electrostatic/gecko-inspired adhesives soft robotic gripper. *IEEE Robotics and Automation Letters*, *5*(3), 4679–4686. https://doi.org/10.1109/LRA.2020.3003773

[14] Autumn, K. (2007). Gecko adhesion: Structure, function, and applications. *MRS Bulletin*, *32*(6), 473–478. https://doi.org/10.1557/MRS2007.80

[15] Autumn, K. (2006). Properties, principles, and parameters of the gecko adhesive system. In A. M. Smith & J. A. Callow (Eds.), *Biological adhesives* (pp. 225-256). Springer. https://doi.org/10.1007/978-3-540-31049-5_12

[16] Autumn, K., & Peattie, A. M. (2002). Mechanisms of adhesion in geckos. *Integrative and Comparative Biology*, *42*(6), 1081–1090. https://doi.org/10.1093/icb/42.6.1081

[17] Basak, S. (2021). Redefining stickiness–A reflection on the gecko inspired adhesives possessing self-cleaning traits. *Journal of Adhesion Science and Technology*, *35*(14), 1473–1491. https://doi.org/10.1080/01694243.2020.1851938

[18] Materzok, T., de Boer, D., Gorb, S., & Müller-Plathe, F. (2022). Gecko adhesion on flat and rough surfaces: Simulations with a multi-scale molecular model. *Small*, *18*(35), 2201674. https://doi.org/10.1002/smll.202201674

[19] Autumn, K., Liang, Y. A., Hsieh, S. T., Zesch, W., Chan, W. P., Kenny, T. W., ..., & Full, R. J. (2000). Adhesive force of a single gecko foot-hair. *Nature*, *405*(6787),681–685. https://doi.org/10.1038/35015073

[20] Ge, L., Sethi, S., Ci, L., Ajayan, P. M., & Dhinojwala, A. (2007). Carbon nanotube-based synthetic gecko tapes. *Proceedings*

of the National Academy of Sciences, *104*(26), 10792–10795. https://doi.org/10.1073/pnas.0703505104

[21] Sethi, S., Ge, L., Ci, L., Ajayan, P. M., & Dhinojwala, A. (2008). Gecko-inspired carbon nanotube-based self-cleaning adhesives. *Nano Letters*, *8*(3), 822–825. https://doi.org/10.1021/nl0727765

[22] Murphy, M. P., Aksak, B., & Sitti, M. (2009). Gecko-inspired directional and controllable adhesion. *Small*, *5*(2), 170–175. https://doi.org/10.1002/smll.200801161

[23] Murphy, M. P., Aksak, B., & Sitti, M. (2007). Adhesion and anisotropic friction enhancements of angled heterogeneous micro-fiber arrays with spherical and spatula tips. *Journal of Adhesion Science and Technology, 21*(12–13), 1281–1296. https://doi.org/10.1163/156856107782328380

[24] Northen, M. T., Greiner, C., Arzt, E., & Turner, K. L. (2008). A gecko-inspired reversible adhesive. *Advanced Materials*, *20*(20), 3905–3909. https://doi.org/10.1002/adma.200801340

[25] Chary, S., Tamelier, J., & Turner, K. (2013). A microfabricated gecko-inspired controllable and reusable dry adhesive. *Smart Materials and Structures*, *22*(2), 025013. http://doi.org/10.1088/0964-1726/22/2/025013

[26] Mengüç, Y., & Sitti, M. (2013). Gecko-inspired polymer adhesives. In H. Zeng (Ed.), *Polymer adhesion, friction, and lubrication* (pp. 351-389). Wiley. https://doi.org/10.1002/9781118505175.CH9

[27] Sitti, M., & Fearing, R. S. (2003). Synthetic gecko foot-hair micro/nano-structures as dry adhesives. *Journal of Adhesion Science and Technology*, *17*(8), 1055–1073. https://doi.org/10.1163/156856103322113788

[28] Shao, Y., Li, M., Tian, H., Zhao, F., Xu, J., Hou, H., ..., & Shao, J. (2025). Gecko-inspired intelligent adhesive structures for rough surfaces. *Research*, *8*, 0630. https://doi.org/10.34133/research.0630

[29] Shi, W., Cheng, X., & Cheng, K. (2022). Gecko-inspired adhesives with asymmetrically tilting-oriented micropillars. *Langmuir*, *38*(29),8890–8898.https://doi.org/10.1021/acs.langmuir.2c01002

[30] Shen, C., Cheng, Y., Peng, Z., & Chen, S. (2024). Switchable adhesion of gecko-inspired hierarchically wedge-mushroom-shaped surface. *Chemical Engineering Journal*, *488*, 150900. https://doi.org/10.1016/j.cej.2024.150900

[31] Pang, C., Wang, Q., Mak, K., Yu, H., & Wang, M. Y. (2022). Viko 2.0: A hierarchical gecko-inspired adhesive gripper with visuotactile sensor. *IEEE Robotics and Automation Letters*, *7*(3), 7842–7849. https://doi.org/10.1109/LRA.2022.3183249

[32] Luo, C., Ma, X., Zhang, Y., Peng, Y., Zhou, Y., Zhao, X., & Zhang, F. (2024). Multiscale synergistic gecko-inspired adhesive for stable adhesion under varying preload and surface roughness. *Langmuir*, *40*(19), 9957–9964. https://doi.org/10.1021/acs.langmuir.4c00064

[33] Kim, S., Spenko, M., Trujillo, S., Heyneman, B., Mattoli, V., & Cutkosky, M. R. (2007). Whole body adhesion: Hierarchical, directional and distributed control of adhesive forces for a climbing robot. In *Proceedings 2007 IEEE International Conference on Robotics and Automation*, 1268–1273. IEEE. https://doi.org/10.1109/ROBOT.2007.363159

[34] Henrey, M., Ahmed, A., Boscariol, P., Shannon, L., & Menon, C. (2014). Abigaille-III: A versatile, bioinspired hexapod for scaling smooth vertical surfaces. *Journal of Bionic Engineering*, *11*(1), 1–17. https://doi.org/10.1016/S1672-6529%2814%2960015-9

[35] Hoang, T. T., Quek, J. J. S., Thai, M. T., Phan, P. T., Lovell, N. H., & Do, T. N. (2021). Soft robotic fabric gripper with gecko adhesion and variable stiffness. *Sensors and Actuators A: Physical*, *323*, 112673. https://doi.org/10.1016/J.SNA.2021.112673

[36] Zhang, Y., Richards, J. T., Hellein, J. L., Johnson, C. M., Woodall, J., Sorenson, T., ..., & Levine, H. G. (2022). NASA's ground-based microgravity simulation facility. In E. B. Blancaflor (Ed.), *Plant gravitropism: Methods and protocols* (pp. 281–299). Springer. https://doi.org/10.1007/978-1-0716-1677-2_18

[37] Sawada, H., Ui, K., Mori, M., Yamamoto, H., Hayashi, R., Matunaga, S., & Ohkami, Y. (2004). Micro-gravity experiment of a space robotic arm using parabolic flight. *Advanced Robotics*, *18*(3), 247–267. https://doi.org/10.1163/156855304322972431

[38] Sun, C., Chen, S., Yuan, J., & Zhu, Z. (2017). A six-DOF buoyancy tank microgravity test bed with active drag compensation. *Microgravity Science and Technology*, *29*(5), 391–402. https://doi.org/10.1007/S12217-017-9554-9

[39] Geordas, C., Chen, H. J., Henbury, S. K., Ingrilli, S. S., Khan, J. I., Rahman, N., & Tanner, P. A. (2022). Implementation of Experimental Microgravity Unit 2 for low-cost and accessible microgravity experimentation. In *73rd International Astronautical Congress*, 1–2.

[40] Hart, S., Sanchez, E., Malik, H., Glenn Lightsey, E., & Romero-Calvo, Á. (2024). Neutral buoyancy testing of low-gravity fluid management. *AIAA Journal*, *62*(2), 858-863. https://doi.org/10.2514/1.j063601

[41] Jairala, J., Durkin, R., Marak, R., Prince, A., Sipila, S., Ney, Z., ..., & Thomason, A. (2012). Extravehicular activity development and verification testing at NASA's Neutral Buoyancy Laboratory. In *42nd International Conference on Environmental Systems*, 1–18. https://doi.org/10.2514/6.2012-3592

[42] Golliher, E. L., Zivich, C. P., & Yao, S. C. (2005). Exploration of unsteady spray cooling for high power electronics at microgravity using NASA Glenn's drop tower. In *Heat Transfer Summer Conference*, 609–612. https://doi.org/10.1115/HT2005-72123

[43] Cagnani, I., Manhard, A., Koenig, C., & Adams, A. (2004). Freefalling balloon launched laboratory for low cost microgravity. In *55th International Astronautical Congress*, 1–7. https://doi.org/10.2514/6.IAC-04-J.5.09

[44] Uno, K., Takada, K., Nagaoka, K., Kato, T., Candalot, A., & Yoshida, K. (2024). Lower gravity demonstratable testbed for space robot experiments. In *2024 IEEE/SICE International Symposium on System Integration*, 1183–1184. https://doi.org/10.1109/SII58957.2024.10417210

[45] Basmadji, F. L., Chmaj, G., Rybus, T., & Seweryn, K. (2019). Microgravity testbed for the development of space robot control systems and the demonstration of orbital maneuvers. In *Photonics Applications in Astronomy, Communications, Industry, and High-Energy Physics Experiments 2019: Proceedings of SPIE*, 11176, 111763V. https://doi.org/10.1117/12.2537981

[46] Liang, P., Gao, X., Zhang, Q., Li, M., Gao, R., & Xu, Y. (2021). Analysis and experimental research on motion stability of wall-climbing robot with double propellers. *Advances in Mechanical Engineering*, *13*(9), 16878140211047726. https://doi.org/10.1177/16878140211047726

[47] Song, Y., Yang, Z., Chang, Y., Yuan, H., & Lin, S. (2024). Design and analysis of a wall-climbing robot with passive compliant mechanisms to adapt variable curvatures walls. *Robotica*, *42*(4), 962–976. https://doi.org/10.1017/S026357472300173X

[48] Hassan, M., Dremann, K., Orosa, A., Metzger, E., Doty, N., Patek, J., ..., & Mahajan, A. (2025). Design and simulation of a four-legged mobile robot for autonomous navigation on

a spacecraft hull. *Journal of Robotics*, *2025*(1), 2542899. https://doi.org/10.1155/joro/2542899

[49] Hassan, M., Mahajan, A., Gao, X., Quinn, D. D., & Farhad, S. (2025). Scalable gecko-inspired adhesives via diffraction-grated molds: A low-cost, directional PDMS system. *Engineering Reports*, *7*(10), e70352. https://doi.org/10.1002/eng2.70352

[50] Lee, S. H., Hwang, I., Kang, B. S., Jeong, H. E., & Kwak, M. K. (2019). Highly flexible and self-adaptive dry adhesive end-effectors for precision robotics. *Soft Matter*, *15*(29), 5827–5834. https://doi.org/10.1039/c9sm00431a

[51] Akinyemi, T. O., Omisore, O. M., Duan, W., Lu, G., Al-Handerish, Y., Han, S., & Wang, L. (2021). Fiber Bragg grating-based force sensing in robot-assisted cardiac interventions: A review. *IEEE Sensors Journal*, *21*(9), 10317–10331. https://doi.org/10.1109/JSEN.2021.3060515

[52] Cao, M. Y., Laws, S., & y Baena, F. R. (2021). Six-axis force/torque sensors for robotics applications: A review. *IEEE Sensors Journal*, *21*(24), 27238–27251. https://doi.org/10.1109/JSEN.2021.3123638

[53] Kim, J. H. (2020). Multi-axis force-torque sensors for measuring zero-moment point in humanoid robots: A review. *IEEE Sensors Journal*, *20*(3), 1126–1141. https://doi.org/10.1109/JSEN.2019.2947719

[54] Gao, Y., Yan, C., Huang, H., Yang, T., Tian, G., Xiong, D., ..., & Yang, W. (2020). Microchannel-confined MXene based flexible piezoresistive multifunctional micro-force sensor. *Advanced Functional Materials*, *30*(11), 1909603. https://doi.org/10.1002/adfm.201909603

[55] Gravish, N., Wilkinson, M., & Autumn, K. (2008). Frictional and elastic energy in gecko adhesive detachment. *Journal of the Royal Society Interface*, *5*(20), 339–348. https://doi.org/10.1098/rsif.2007.1077

[56] Santos, D., Kim, S., Spenko, M., Parness, A., & Cutkosky, M. (2007). Directional adhesive structures for controlled climbing on smooth vertical surfaces. In *Proceedings 2007 IEEE International Conference on Robotics and Automation*, 1262–1267. https://doi.org/10.1109/ROBOT.2007.363158

[57] Mi, Y., Niu, Y., Ni, H., Zhang, Y., Wang, L., Liu, Y., ..., & Xu, Q. (2022).Gecko inspired reversible adhesion via quantum dots enabled photo-detachment. *Chemical Engineering Journal*, *431*, 134081. https://doi.org/10.1016/j.cej.2021.134081

[58] Wang, B., Xiong, X., Duan, J., Wang, Z., & Dai, Z. (2021). Compliant detachment of wall-climbing robot unaffected by adhesion state. *Applied Sciences*, *11*(13), 5860. https://doi.org/10.3390/app11135860

[59] Wang, H., Yamamoto, A., & Higuchi, T. (2014). A crawler climbing robot integrating electroadhesion and electrostatic actuation. *International Journal of Advanced Robotic Systems*, *2014*(12), 191. https://doi.org/10.5772/59118

[60] Han, A. K., Hajj-Ahmad, A., & Cutkosky, M. R. (2021). Hybrid electrostatic and gecko-inspired gripping pads for manipulating bulky, non-smooth items. *Smart Materials and Structures*, *30*(2), 025010. https://doi.org/10.1088/1361-665X%2Fabca51

[61] Wang, J., Wan, Y., Wang, X., & Xia, Z. (2021). Bioinspired smart materials with externally-stimulated switchable adhesion. *Frontiers in Nanotechnology*, *3*, 667287. https://doi.org/10.3389/fnano.2021.667287

[62] Park, J. E., Won, S., Cho, W., Kim, J. G., Jhang, S., Lee, J. G., & Wie, J. J. (2021). Fabrication and applications of stimuli-responsive micro/nanopillar arrays. *Journal of Polymer Science*, *59*(14), 1491–1517. https://doi.org/10.1002/POL.20210311

[63] Murphy, M. P., Kim, S., & Sitti, M. (2009). Enhanced adhesion by gecko-inspired hierarchical fibrillar adhesives. *ACS Applied Materials & Interfaces*, *1*(4), 849-855. https://doi.org/10.1021/am8002439

[64] Shao, D., Chen, J., Ji, A., Dai, Z., & Manoonpong, P. (2020). Hybrid soft-rigid foot with dry adhesive material designed for a gecko-inspired climbing robot. In *2020 3rd IEEE International Conference on Soft Robotics*, 578–585. https://doi.org/10.1109/RoboSoft48309.2020.9116045

[65] Tang, Y., Zhang, Q., Lin, G., & Yin, J. (2018). Switchable adhesion actuator for amphibious climbing soft robot. *Soft robotics*, *5*(5), 592–600. https://doi.org/10.1089/soro.2017.0133

[66] Kim, S., Spenko, M., Trujillo, S., Heyneman, B., Santos, D., & Cutkosky, M. R. (2008). Smooth vertical surface climbing with directional adhesion. *IEEE Transactions on robotics*, *24*(1), 65–74.

[67] Higham, T. E., & Russell, A. P. (2025). Geckos running with dynamic adhesion: towards integration of ecology, energetics and biomechanics. *Journal of Experimental Biology*, *228*(Suppl_1), JEB247980. https://doi.org/10.1242/jeb.247980

[68] Zhang, Y., Qian, Y., Ding, Y., Hou, B., & Wang, R. (2023). Adaptive walking control for quadruped robot by using oscillation patterns. *Scientific Reports*, *13*(1), 19756. https://doi.org/10.1038/s41598-023-47022-x

[69] Akkawutvanich, C., Knudsen, F. I., Riis, A. F., Larsen, J. C., & Manoonpong, P. (2020). Adaptive parallel reflex-and decoupled CPG-based control for complex bipedal locomotion. *Robotics and Autonomous Systems*, *134*, 103663. https://doi.org/10.1016/J.ROBOT.2020.103663

[70] Ouyang, W., Chi, H., Pang, J., Liang, W., & Ren, Q. (2021). Adaptive locomotion control of a hexapod robot via bio-inspired learning. *Frontiers in Neurorobotics*, *15*, 627157. https://doi.org/10.3389/fnbot.2021.627157

[71] Huang, X., Wu, C., Xiang, H., Liang, R., Funabora, Y., & Peng, Y. (2025). Bio-inspired soft pipeline robot with origami-based adaptive guidance. In *2025 IEEE International Conference on Mechatronics and Automation*, 1260–1265. https://doi.org/10.1109/ICMA65362.2025.11120689

[72] Peng, Y., Nabae, H., Funabora, Y., & Suzumori, K. (2024). Peristaltic transporting device inspired by large intestine structure. *Sensors and Actuators A: Physical*, *365*, 114840. https://doi.org/10.1016/j.sna.2023.114840

[73] Bae, W. G., Kim, H. N., Kim, D., Park, S. H., Jeong, H. E., & Suh, K. Y. (2014). Scalable multiscale patterned structures inspired by nature: The role of hierarchy. *Advanced Materials*, *26*(5), 675–700. https://doi.org/10.1002/adma.201303412

[74] Tang, T., Ahire, B., & Li, X. (2023). Scalable multi-material additive manufacturing of bioinspired polymeric material with metallic structures via electrically assisted stereolithography. *Journal of Manufacturing Science and Engineering*, *145*(1), 011004. https://doi.org/10.1115/1.4055793

How to Cite: Hassan, M., Fayomi, O., Faust, J., & Mahajan, A. (2025). A Bio-inspired Climbing Robot with Directional Dry Adhesion for Reduced-Gravity Mobility. *Journal of Climbing and Walking Robots*. https://doi.org/10.47852/bonviewJCWR52026892